

This is a repository copy of *Establishing the Maximum Collectivity in Highly Deformed N=Z Nuclei*.

White Rose Research Online URL for this paper:

<https://eprints.whiterose.ac.uk/id/eprint/160432/>

Version: Published Version

---

**Article:**

Llewellyn, R D O, Bentley, M A [orcid.org/0000-0001-8401-3455](https://orcid.org/0000-0001-8401-3455), Wadsworth, R [orcid.org/0000-0002-4187-3102](https://orcid.org/0000-0002-4187-3102) et al. (24 more authors) (2020) Establishing the Maximum Collectivity in Highly Deformed N=Z Nuclei. *Physical Review Letters*. 152501. ISSN: 1079-7114

<https://doi.org/10.1103/PhysRevLett.124.152501>

---

**Reuse**

Items deposited in White Rose Research Online are protected by copyright, with all rights reserved unless indicated otherwise. They may be downloaded and/or printed for private study, or other acts as permitted by national copyright laws. The publisher or other rights holders may allow further reproduction and re-use of the full text version. This is indicated by the licence information on the White Rose Research Online record for the item.

**Takedown**

If you consider content in White Rose Research Online to be in breach of UK law, please notify us by emailing [eprints@whiterose.ac.uk](mailto:eprints@whiterose.ac.uk) including the URL of the record and the reason for the withdrawal request.

# Establishing the Maximum Collectivity in Highly Deformed $N = Z$ Nuclei

R. D. O. Llewellyn<sup>1,\*</sup>, M. A. Bentley<sup>1</sup>, R. Wadsworth<sup>1,†</sup>, H. Iwasaki<sup>2,3</sup>, J. Dobaczewski<sup>1,4</sup>, G. de Angelis<sup>5</sup>, J. Ash<sup>2,3</sup>, D. Bazin<sup>2,3</sup>, P. C. Bender<sup>2,‡</sup>, B. Cederwall<sup>6</sup>, B. P. Crider<sup>2,§</sup>, M. Doncel<sup>7</sup>, R. Elder<sup>2,3</sup>, B. Elman<sup>2,3</sup>, A. Gade<sup>2,3</sup>, M. Grinder<sup>2,3</sup>, T. Haylett<sup>1</sup>, D. G. Jenkins<sup>1</sup>, I. Y. Lee<sup>8</sup>, B. Longfellow<sup>2,3</sup>, E. Lunderberg<sup>2,3</sup>, T. Mijatović<sup>2,||</sup>, S. A. Milne<sup>1</sup>, D. Muir<sup>1</sup>, A. Pastore<sup>1</sup>, D. Rhodes<sup>2,3</sup>, and D. Weisshaar<sup>2</sup>

<sup>1</sup>*Department of Physics, University of York, Heslington, York YO10 5DD, United Kingdom*

<sup>2</sup>*National Superconducting Cyclotron Laboratory, Michigan State University, East Lansing, Michigan 48824, USA*

<sup>3</sup>*Department of Physics and Astronomy, Michigan State University, East Lansing, Michigan 48824, USA*

<sup>4</sup>*Institute of Theoretical Physics, Faculty of Physics, University of Warsaw, ul. Pasteura 5, PL-02-093 Warsaw, Poland*

<sup>5</sup>*Legnaro National Laboratory, 35020 Legnaro, Italy*

<sup>6</sup>*KTH Department of Physics, S-10691 Stockholm, Sweden*

<sup>7</sup>*Department of Physics, University of Liverpool, Liverpool L69 3BX, United Kingdom*

<sup>8</sup>*Nuclear Science Division, Lawrence Berkeley National Laboratory, Berkeley, California 94720, USA*



(Received 7 October 2019; accepted 18 March 2020; published 16 April 2020)

The lifetimes of the first excited  $2^+$  states in the  $N = Z$  nuclei  $^{80}\text{Zr}$ ,  $^{78}\text{Y}$ , and  $^{76}\text{Sr}$  have been measured using the  $\gamma$ -ray line shape method following population via nucleon-knockout reactions from intermediate-energy rare-isotope beams. The extracted reduced electromagnetic transition strengths yield new information on where the collectivity is maximized and provide evidence for a significant, and as yet unexplained, odd-odd vs even-even staggering in the observed values. The experimental results are analyzed in the context of state-of-the-art nuclear density-functional model calculations.

DOI: [10.1103/PhysRevLett.124.152501](https://doi.org/10.1103/PhysRevLett.124.152501)

The basic understanding of why atomic nuclei possess different shapes as a function of isospin and excitation energy relies heavily on experimental data identifying new physics phenomena and on developments in nuclear theory to explain and predict such properties. The development of nuclear collectivity (related to deformation) is a key property central to our understanding of the nuclear force.

Self-conjugate ( $N = Z$ ) nuclei in the mass ( $A$ ) 80 region are predicted to possess some of the most deformed ground states of all nuclei in nature [1–4]. The reduced transition probability  $B(E2; 2^+ \rightarrow 0^+)$  [denoted  $B(E2\downarrow)$ ] is one of the best probes of quadrupole collectivity and provides an indication of nuclear deformation.  $B(E2\downarrow)$  values exist for the medium-heavy  $N = Z$  nuclei  $^{64}\text{Ge}$  [5],  $^{68}\text{Se}$  [6,7],  $^{70}\text{Br}$  [7],  $^{72}\text{Kr}$  [8,9],  $^{74}\text{Rb}$  [10], and  $^{76}\text{Sr}$  [11]. These demonstrate rapidly increasing nuclear collectivity with the addition of nucleons beyond  $A > 70$ . This rapid variation makes this an attractive region to test nuclear models. The remarkably low  $E(2^+)$  energies of the  $N = Z$  nuclei  $^{76}\text{Sr}$  [12],  $^{78}\text{Y}$  [13], and  $^{80}\text{Zr}$  [14] are indicative of the neutron-deficient  $A \approx 80$  region being strongly deformed, a compelling suggestion of enhanced collectivity. Beyond mean field methods calculations predict  $^{80}\text{Zr}$  to exhibit five different, almost degenerate, nuclear shapes. These calculations suggest that the ground state possesses a near-axial highly deformed shape with  $\beta_2 = 0.55$  and  $B(E2\downarrow) = 3900 e^2 \text{fm}^4$  [15]. Given that  $B(E2\downarrow) = 2220(270) e^2 \text{fm}^4$  has been measured

for  $^{76}\text{Sr}$  [11], corresponding to a smaller deformation of  $\beta_2 = 0.45(3)$ , further measurements are clearly needed to establish the experimental trend of the collectivity in  $N = Z$  nuclei up to, and beyond, the midpoint between the spherical doubly closed-shell  $N = Z$  nuclei  $^{56}\text{Ni}$  and  $^{100}\text{Sn}$ .

$N = Z$  nuclei play a pivotal role when investigating neutron-proton (np) collectivity due to the spatial overlap of their respective wave functions at the Fermi surface, allowing them to act coherently. This can result in isoscalar (isospin  $T = 0$ , coupled angular momentum  $I > 0$ ) fermion np pairs [16,17]; a feature unique to nuclei. It has been hypothesized that a nuclear superfluid [18–21], analogous to “Cooper Pairs” in superconductors, exists in nuclei with competing isoscalar np pairing and normal (np and like-nucleon, nn and pp) isovector ( $T = 1, I = 0$ ) pairing modes. The former has been predicted to become more prominent in the ground states of heavier ( $A > 76$ )  $N = Z$  nuclei [22] and to play an important role at higher spins in  $^{80}\text{Zr}$  [23]. Despite there being no conclusive experimental evidence of this specific phenomenon, shell-model calculations predict that isoscalar pairing has an important role in enhancing collectivity in heavier  $N = Z$  nuclei [24]. Hence, measurements of  $B(E2\downarrow)$  in these nuclei are important.

The present work has determined the mean lifetimes of the first  $2^+$  states in  $^{76}\text{Sr}$ ,  $^{78}\text{Y}$ , and  $^{80}\text{Zr}$ , yielding the first data at and beyond the midshell point between  $^{56}\text{Ni}$  and  $^{100}\text{Sn}$ . The new data also reveals the presence of a clear

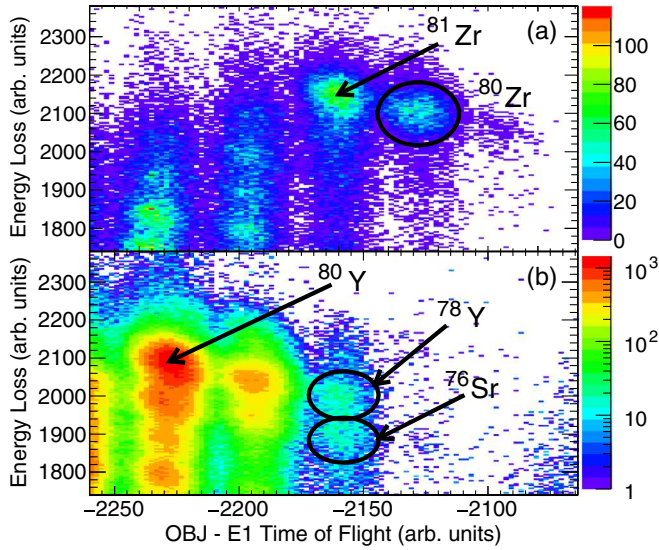


FIG. 1. Particle identification of reaction products from the (a)  $^{81}_{40}\text{Zr}$  and (b)  $^{80}_{39}\text{Y}$  secondary beams. The plot shows energy loss against time of flight measurements from the detection system of the S800 spectrograph focal plane.

staggering effect in the  $B(E2\downarrow)$  values between odd-odd and even-even nuclei, which cannot be explained using state-of-the-art density functional theory (DFT) calculations including standard isovector pairing.

The experiment, performed at the National Superconducting Cyclotron Laboratory (NSCL) at Michigan State University, utilized a  $^{92}\text{Mo}$  primary beam at an energy of 140 MeV/nucleon following acceleration by the K500 and K1200 cyclotrons [25]. A cocktail of secondary beams was produced following fragmentation on a thick  $^9\text{Be}$  target at the entrance to the A1900 separator [26]. The extracted cocktail beam consisted of  $\approx 0.9\%$   $^{81}\text{Zr}$ ,  $\approx 8.5\%$   $^{80}\text{Y}$ ,  $\approx 26.8\%$   $^{79}\text{Sr}$ ,  $\approx 43.3\%$   $^{78}\text{Rb}$ , and  $\approx 18.9\%$   $^{77}\text{Kr}$ . The  $2^+$  state of the  $N = Z$   $^{80}_{40}\text{Zr}$  was populated via one-neutron knockout from the  $\sim 400$  pp s  $^{81}_{40}\text{Zr}$  secondary beam with an energy of 77 MeV/nucleon [Fig. 1(a)], while the  $2^+$  state in  $^{78}_{38}\text{Sr}$  was populated via one-neutron knockout from  $^{79}_{38}\text{Sr}$ . The nuclei  $^{78}_{39}\text{Y}$  and  $^{76}_{38}\text{Sr}$  were both populated through the  $^{80}_{39}\text{Y}$  secondary beam, via two-neutron knockout and three-neutron, one-proton removal reactions, respectively [Fig. 1(b)].

The secondary beams were separated via the A1900 separator with a momentum acceptance of 0.5% prior to impinging on a 188-mg/cm<sup>2</sup>-thick  $^9\text{Be}$  target at the S800 target position. Products of the knockout reactions from each secondary beam were identified via time-of-flight and energy-loss measurements, with corrections for position and angle dependence using the ion track information from the S800 spectrograph [27]. In-flight de-excitation  $\gamma$  rays of reaction products at the secondary  $^9\text{Be}$  target position, were detected with the Gamma-Ray Energy Tracking In-beam Nuclear Array (GRETINA) [28]. GRETINA consisted of two rings with four detector modules centered at 58° and six

at 90°, covering laboratory angles of 37° to 116°, with each module consisting of four 36-fold segmented HPGe crystals.

Lifetimes of the  $2^+$  states in  $^{80}\text{Zr}$ ,  $^{78}\text{Y}$ ,  $^{78}\text{Sr}$ , and  $^{76}\text{Sr}$  were obtained using an established  $\gamma$ -ray line shape method [29,30], previously used to measure lifetimes of states in  $^{53}\text{Ni}$  [31],  $^{78}\text{Sr}$ , and  $^{76}\text{Sr}$  [11]. This method utilizes the position distribution of the reaction products downstream of the target position at the time of de-excitation. At beam velocities appropriate to the present experiment ( $v/c = 0.3$ ), this corresponds to  $\approx 0.9$  cm downstream of the target position per 100 ps. The resulting low-energy tails of the event-by-event Doppler-corrected  $\gamma$ -ray spectra were replicated through GEANT4 simulations incorporating both the S800 spectrograph and GRETINA geometries [32]. The lifetime, energy, and scale of the simulated  $2^+ \rightarrow 0^+$  transitions and an exponential background contribution were allowed to vary freely until the  $\chi^2$  of the simulation compared to the experimental spectrum was minimized. The GRETINA lifetime simulation package allows for effects on the  $\gamma$ -ray line shape resulting from transitions feeding the  $2^+$  state. Lifetimes from the feeding  $4^+ \rightarrow 2^+$  transitions were estimated from the known lifetime of the  $4^+$  state in  $^{78}\text{Sr}$  [33], scaled by a factor of  $1/E_\gamma^5$ . Effects of this feeding on the measured  $2^+$  lifetimes is small given that the  $4^+ \rightarrow 2^+$  decay is  $> 20$  times faster. To confirm the veracity of the method we have measured the lifetime of the  $2^+$  state in  $^{78}\text{Sr}$  to compare with the known value [11].

The lifetime and energy of the  $2^+$  states were determined through a 2D  $\chi^2$ -minimization procedure, replicating the method used in Ref. [31]. Allowing the energy of the  $2^+ \rightarrow 0^+$  transition to vary freely eliminates any systematic uncertainties, when determining the optimum lifetime, arising from imperfect geometry or Doppler correction or previous  $\gamma$ -ray energy determination. Doppler-corrected spectra for  $^{80}\text{Zr}$ ,  $^{78}\text{Y}$ ,  $^{78}\text{Sr}$ , and  $^{76}\text{Sr}$  are displayed in Fig. 2 with the optimized simulations. The corresponding  $\chi^2$  distributions for lifetime, having minimized already on the energy, are shown in the inset. The small, high-energy tail observable in the peaks for  $^{80}\text{Zr}$  and  $^{78}\text{Sr}$  [Figs. 2(a) and 2(c)] is due to incorrect reconstruction of a small number of events by GRETINA. A similar low-energy tail should also be present, but has no effect on the extracted lifetime since the spectral shape is dominated by Doppler-line shape effects. Since there is no simple way of simulating this effect, the 294–300 keV region was excluded from the  $\chi^2$ -minimization procedure for  $^{80}\text{Zr}$ . This reduced the total  $\chi^2$  but had no effect on the measured lifetime. The statistical error of the mean lifetime is derived from the  $\chi^2 + 1$  value of the fitted  $\chi^2$ -distribution minimum, yielding  $^{-10}_{+10}$  ps for  $^{80}\text{Zr}$ . Systematic errors arise from uncertainties in beam velocity (varies depending on nucleus), exponential background (0.1%), simulated GRETINA interaction position resolution (6.2%), effects of states feeding into the  $2^+$  state

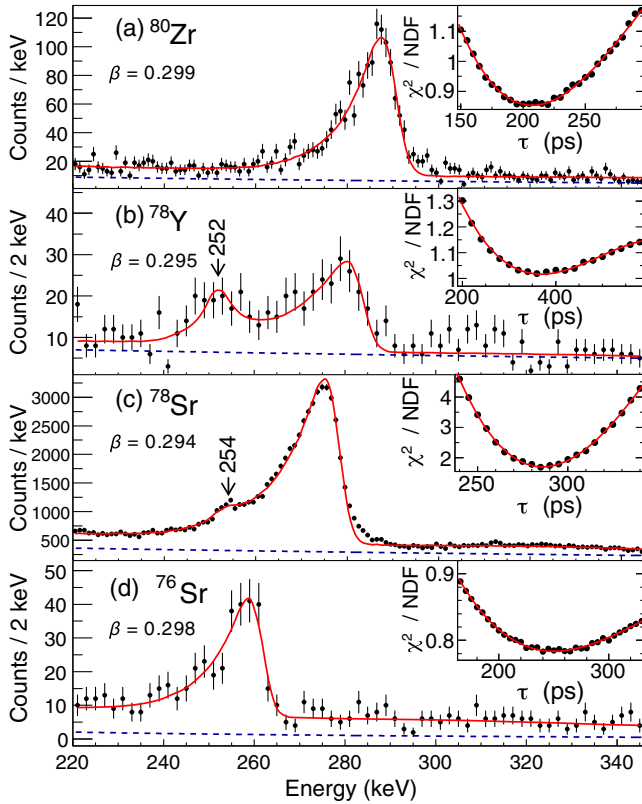


FIG. 2. Doppler-shift corrected  $\gamma$ -ray spectra for (a)  $^{80}\text{Zr}$ , (b)  $^{78}\text{Y}$ , (c)  $^{78}\text{Sr}$ , and (d)  $^{76}\text{Sr}$  at the specified after-target velocity ( $\beta$ ). Experimental spectra are compared to the optimum simulated spectra (red lines) with an additional exponential background contribution (dashed blue lines). Inset plots display the  $\chi^2$  per number of degrees of freedom (NDF) distributions as a function of mean lifetime at the optimum energy determined through the 2D  $\chi^2$ -minimization procedure employed (see text), with the minima corresponding to the measured lifetime.

(varies),  $\gamma$ -ray anisotropy effects (1.5%) and geometrical uncertainties (3%). Combining these in quadrature produces a mean lifetime for  $^{80}\text{Zr}$  of  $\tau = 207(19)$  ps at an energy of  $E(2^+) = 290.4(4)$  keV yielding  $B(E2\downarrow) = 1910(180) e^2 \text{fm}^4$ . All results are summarized in Table I.

The identical procedure was repeated for  $^{78}\text{Sr}$  to ensure that a lifetime consistent with that of Ref. [11] was obtained. The known 254 keV  $5^- \rightarrow 4^-$  transition [34] is observed within the line shape of  $^{78}\text{Sr}$  [Fig. 2(c)], which was included within the simulation with a short lifetime of 1 ps, where its energy and intensity were allowed to vary freely. As with  $^{80}\text{Zr}$ , the upper-tail region between 280–290 keV was excluded from the fit. The statistical error of  $\pm 3$  ps was combined with the aforementioned systematic errors giving a mean lifetime of  $\tau = 286(20)$  ps and an energy of  $E(2^+) = 278.1(3)$  keV. This agrees with  $\tau = 276(39)$  ps from Ref. [11] and is consistent with the earlier measurement of Ref. [33]. The weighted average of these results produces a value for  $B(E2\downarrow)$  of  $1840(100) e^2 \text{fm}^4$ . The same procedure produces

TABLE I. Optimum  $E(2^+)$  energies in keV and mean lifetimes  $\tau$  in ps extracted from the  $\chi^2$ -minimization procedure.  $E(2^+)$  errors are calculated from statistical and systematic uncertainties (see text for details). The measured mean lifetimes are compared with previously measured values ( $\tau_{\text{prev}}$ ) where possible. Weighted averages for the mean lifetimes ( $\tau_{\text{avg}}$ ) are then used to calculate  $B(E2\downarrow)$  values in  $e^2 \text{fm}^4$ .

	$E(2^+)$	$\tau$	$\tau_{\text{prev},1}$	$\tau_{\text{prev},2}$	$\tau_{\text{avg}}$	$B(E2\downarrow)$
$^{80}\text{Zr}$	290.4(4)	207(19)				1910(180)
$^{78}\text{Y}$	283.6(8)	$369^{+77}_{-54}$				$1200^{+180}_{-250}$
$^{78}\text{Sr}$	278.1(3)	286(20)	$276(39)^a$	$224(27)^b$	266(15)	1840(100)
$^{76}\text{Sr}$	261.6(5)	250(44)	$296(36)^a$		278(28)	2390(240)

<sup>a</sup>Reference [11].

<sup>b</sup>Reference [33].

$\tau = 250(44)$  ps for the  $2^+$  state of  $^{76}\text{Sr}$  at  $E(2^+) = 261.6(5)$  keV [Fig. 2(d)], which are consistent with the known values of 261.5(3) keV [35] and 296(36) ps [11]. The weighted average of these values produces  $B(E2\downarrow) = 2390(240) e^2 \text{fm}^4$ .

In the case of  $^{78}\text{Y}$  [Fig. 2(b)], an unknown  $\sim 252$  keV transition is seen in the line shape. Due to low statistics, it was not possible to confirm if this decay is coincident with the  $2^+ \rightarrow 0^+$  transition. It is also possible that this contaminant possesses a sufficiently long lifetime ( $\gtrsim 50$  ps) to impact the line shape. Allowing the lifetime of the state that emits the  $\gamma$  ray to vary from 1 to 100 ps, whilst allowing the contaminant's intensity to vary, introduces an additional systematic error of  $^{+50}_{-0}$  ps on the  $2^+$  lifetime. Likewise, lowering or raising the contaminant's energy by 1 keV with a lifetime of 1 ps yields an average systematic error of  $^{+27}_{-0}$  ps, culminating to a total systematic error, when combined with the previously mentioned factors, of  $^{+59}_{-31}$  ps. Combined with the statistical error of  $^{+49}_{-44}$  ps, a mean lifetime of  $\tau = 369^{+77}_{-54}$  ps at  $E(2^+) = 283.6(8)$  keV is obtained, corresponding to a  $B(E2\downarrow)$  of  $1200^{+180}_{-250} e^2 \text{fm}^4$ . A small discrepancy exists between the extracted  $\gamma$ -ray energy and that of Ref. [13] (281 keV), however, the latter was a very low-statistics measurement with no given error.

The systematic behavior of the  $B(E2\downarrow)$  values of the  $N = Z$  nuclei from  $^{64}\text{Ge}$  to  $^{80}\text{Zr}$  is plotted in Fig. 3. There have been various theoretical attempts to replicate the  $B(E2\downarrow)$  systematics of the even-even  $N = Z$  nuclei approaching  $A = 80$ . In a shell-model approach (e.g., Ref. [36]), the large  $fpgds$  model space required in this deformed region provides computational challenges. In particular, severe truncation is required, limiting the ability to reproduce the correct degree of collectivity, and a consistent treatment of  $B(E2\downarrow)$  values across the whole region is hampered by the need for different truncations, valence spaces and interactions. DFT calculations do not suffer from the same limitations. Constrained-Hartree-Fock-Bogoliubov calculations, mapped to the five-dimensional collective



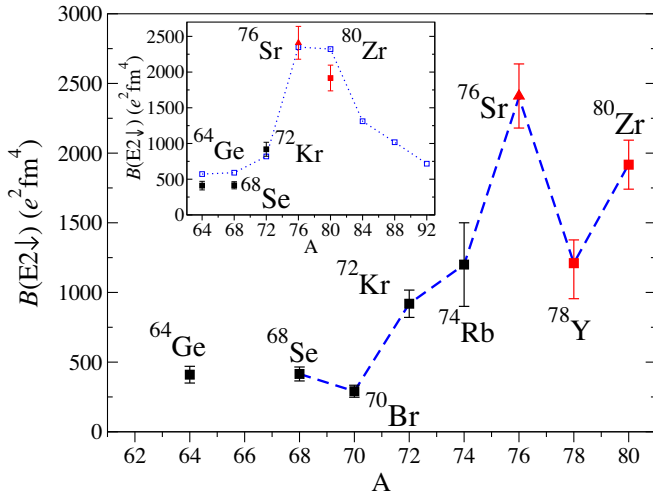


FIG. 3. Schematics of the  $B(E2\downarrow)$  values for the  $N = Z$  nuclei from  $^{64}\text{Ge}$  to  $^{80}\text{Zr}$ . Red symbols correspond to the present work, where  $^{76}\text{Sr}$  (triangle) is a weighted average of the present work and Ref. [11]. The black data points are taken from [5–10] with weighted averages used where possible. The blue dashed line is to guide the eye. The inset displays CHFB + 5DCH calculations from Ref. [1] (blue dotted line) and data for the even-even  $N = Z$  nuclei.

quadrupole Hamiltonian (CHFB + 5DCH) [1], for the even-even  $N = Z$  nuclei are compared to experimental values in the inset of Fig. 3. These incorporate factors such as the mixing of different shapes, including the triaxial degree of freedom. This methodology reproduces the sharp increase in collectivity between  $^{68}\text{Se}$  and  $^{76}\text{Sr}$ , attributed to the  $gd$  orbitals [36–38]. These calculations also show reasonable agreement with the data for  $^{80}\text{Zr}$  and the suggestion that the maximum collectivity is observed in  $^{76}\text{Sr}$ .

The low  $B(E2\downarrow)$  of  $^{78}\text{Y}$  is intriguing since it provides further evidence for an odd-odd vs even-even staggering effect first noticed in  $^{70}\text{Br}$  [7]. The rapidly changing nuclear shapes and collectivity between  $^{68}\text{Se}$  and  $^{76}\text{Sr}$  (see Fig. 3) create challenges when performing calculations to explain the staggering effect in this region. However, for  $^{76}\text{Sr}$  and  $^{80}\text{Zr}$  the more stable collectivity makes DFT approaches potentially more viable. Regarding the  $B(E2\downarrow)$  staggering, there is the possibility of a local nuclear structure origin of this effect, associated with pair blocking [39]. This is important since, in a deformed shell-model (Nilsson) picture, the downsloping (deformation-increasing)  $[422]5/2$  and up-sloping (deformation-decreasing)  $[301]3/2$  orbitals converge at the Fermi level (see Fig. 4). Exploring this possibility, we have performed HFB calculations utilizing the Skyrme UNEDF0 functional [40], where pairing strengths were increased by 20% accounting for the absence of the Lipkin-Nogami approximation. Wave functions of the resulting fully projected states were used to extract  $B(E2\downarrow)$  values for  $^{76}\text{Sr}$  and  $^{80}\text{Zr}$  and are compared with the data in the right-hand panel of Fig. 4 with excellent

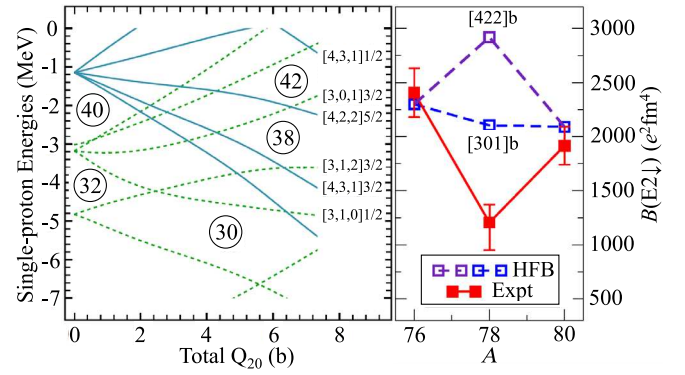


FIG. 4. The left-hand panel displays the calculated Nilsson model single-proton energies against total quadrupole moment (total  $Q_{20}$ ). The circled numbers correspond to gaps between orbitals for a given number of protons. Since  $^{78}\text{Y}$  has an equal number of neutrons and protons, the single-neutron energies are very similar. The Fermi level of  $^{78}\text{Y}$  is at the crossing point of the  $[422]5/2$  and  $[301]3/2$  levels. The effects of blocking each of these orbitals on the  $B(E2\downarrow)$  calculated through HFB calculations (see text) is displayed in the right-hand panel.

agreement. For the odd-odd  $^{78}\text{Y}$ , in the absence of blocking effects, the  $[422]5/2$  and  $[301]3/2$  neutron and proton quasiparticle levels were found to be degenerate and equally occupied. However, blocking a proton and neutron in either quasiparticle level significantly reduces the pairing correlations. As a result, the blocking of the downsloping  $[422]5/2$  level has the net effect of increasing its occupation, whilst simultaneously removing the occupation of the upsloping  $[301]3/2$  level. Both this and the reduction in pairing are deformation-increasing effects and the resulting increase in the  $B(E2\downarrow)$  is seen in Fig. 4. Likewise, blocking the  $[301]3/2$  level results in a decrease in  $B(E2\downarrow)$ . However, in this case, the decrease of pairing correlations in the even-even core cancels any resulting  $B(E2\downarrow)$  reduction almost completely. Hence, despite the deformation-reducing effect of the blocked  $[301]3/2$  orbital, the experimentally-observed  $B(E2\downarrow)$  staggering for  $^{78}\text{Y}$  is not reproduced. A full search at smaller triaxial and oblate deformations fails to find any blocked, stable solutions explaining this effect. However, the possibility of obtaining, for another functional, a specific odd-odd vs even-even staggering cannot be excluded. These calculations utilized standard  $T = 1$  pairing correlations so it is possible that the  $B(E2\downarrow)$  staggering may be a consequence of  $T = 0$  pairing modes, currently not included within DFT calculations.

We note that all early [41] and more advanced [18,22,23] HFB calculations involving  $T = 0$  pairing made specific approximations, in particular, they assumed that particle-hole proton and neutron mean fields were separated from one another. However, a proper self-consistent approach based on the proton-neutron paired quasiparticle wave function [17] stipulates that proton and neutron wave

functions and mean-fields must be mixed [42–44]. Such an extension, which has never been implemented, constitutes a major overhaul of realistic HFB codes and is the subject of our current work. We hope that a correct mean-field treatment of the  $T = 0$  pairing will give us insight into the collectivity of heavy  $N = Z$  nuclei, which was experimentally addressed in this Letter.

In summary,  $B(E2\downarrow)$  values extracted from lifetime measurements of the first  $2^+$  states in  $^{78}\text{Y}$  and  $^{80}\text{Zr}$  extend the picture of the evolution of collectivity along the  $N = Z$  line towards  $^{100}\text{Sn}$ . Experimentally, the maximum collectivity is established to occur at  $^{76}\text{Sr}$ . The observed  $B(E2\downarrow)$  staggering effect provides an indication of a phenomenon in odd-odd  $N = Z$  nuclei that cannot be reproduced by state-of-the-art DFT calculations containing standard isovector ( $T = 1$ ) pairing. The next steps are to extend  $B(E2\downarrow)$  measurements along the  $N = Z$  line to determine if a continuation of this staggering effect is observed. Further theoretical developments following recent progress in HFB DFT calculations with the inclusion of mixing between  $T = 0$  and  $T = 1$  np pairing correlations [17] should provide insight as to whether the  $B(E2\downarrow)$  staggering can be attributed to the presence of isoscalar ( $T = 0$ ) np pairing.

This work was carried out at the National Superconducting Cyclotron Laboratory facility at MSU. The work was supported in part by STFC Grants No. ST/M006433/1, No. ST/L005727/1, and No. ST/P003885/1, the National Science Foundation (NSF) under Grant No. PHY-1565546, the Department of Energy (DOE) under Grant No. DE-SC0020451, the DOE National Nuclear Security Administration through the Nuclear Science and Security Consortium under Award No. DE-NA0003180 and the Polish National Science Centre under Contract No. 2018/31/B/ST2/02220. GREYNA was funded by the DOE, Office of Science. Operation of the array at NSCL was supported by DOE under Grants No. DE-SC0014537 (NSCL) and No. DE-AC02-05CH11231 (LBNL). We acknowledge the CSC-IT Center for Science Ltd., Finland, for the allocation of computational resources.

\*ryan.llewellyn@york.ac.uk

†bob.wadsworth@york.ac.uk

‡Present address: Department of Physics, University of Massachusetts Lowell, Lowell, Massachusetts 01854, USA.

§Present address: Department of Physics and Astronomy, Mississippi State University, Mississippi State, Mississippi 39762, USA.

||Present address: Ruder Bošković Institute, HR-10.001 Zagreb, Croatia.

[1] J. P. Delaroche, M. Girod, J. Libert, H. Goutte, S. Hilaire, S. Péru, N. Pillet, and G. F. Bertsch, *Phys. Rev. C* **81**, 014303 (2010).

- [2] J. Erler, N. Birge, M. Kortelainen, W. Nazarewicz, E. Olsen, A. M. Perhac, and M. Stoitsov, *Nature (London)* **486**, 509 (2012).
- [3] S. E. Agbemava, A. V. Afanasjev, D. Ray, and P. Ring, *Phys. Rev. C* **89**, 054320 (2014).
- [4] P. Möller, A. J. Sierk, T. Ichikawa, and H. Sagawa, *At. Data Nucl. Data Tables* **109–110**, 1 (2016).
- [5] K. Starosta, A. Dewald, A. Dunomes, P. Adrich, A. M. Amthor, T. Baumann, D. Bazin, M. Bowen, B. A. Brown, A. Chester *et al.*, *Phys. Rev. Lett.* **99**, 042503 (2007).
- [6] A. Obertelli, T. Baugher, D. Bazin, J. P. Delaroche, F. Flavigny, A. Gade, M. Girod, T. Glasmacher, A. Goergen, G. F. Grinyer *et al.*, *Phys. Rev. C* **80**, 031304(R) (2009).
- [7] A. J. Nichols, R. Wadsworth, H. Iwasaki, K. Kaneko, A. Lemasson, G. de Angelis, V. Bader, T. Baugher, D. Bazin, M. Bentley *et al.*, *Phys. Lett. B* **733**, 52 (2014).
- [8] A. Gade, D. Bazin, A. Becerril, C. M. Campbell, J. M. Cook, D. J. Dean, D.-C. Dinca, T. Glasmacher, G. W. Hitt, M. E. Howard *et al.*, *Phys. Rev. Lett.* **95**, 022502 (2005).
- [9] H. Iwasaki, A. Lemasson, C. Morse, A. Dewald, T. Braunroth, V. M. Bader, T. Baugher, D. Bazin, J. S. Berryman, C. M. Campbell *et al.*, *Phys. Rev. Lett.* **112**, 142502 (2014).
- [10] C. Morse, H. Iwasaki, A. Lemasson, A. Dewald, T. Braunroth, V. Bader, T. Baugher, D. Bazin, J. Berryman, C. Campbell *et al.*, *Phys. Lett. B* **787**, 198 (2018).
- [11] A. Lemasson, H. Iwasaki, C. Morse, D. Bazin, T. Baugher, J. S. Berryman, A. Dewald, C. Fransen, A. Gade, S. McDaniel *et al.*, *Phys. Rev. C* **85**, 041303(R) (2012).
- [12] P. J. Davies, A. V. Afanasjev, R. Wadsworth, C. Andreoiu, R. A. E. Austin, M. P. Carpenter, D. Dashdorj, S. J. Freeman, P. E. Garrett, A. Görgen *et al.*, *Phys. Rev. C* **75**, 011302(R) (2007).
- [13] B. S. Nara Singh, A. N. Steer, D. G. Jenkins, R. Wadsworth, M. A. Bentley, P. J. Davies, R. Glover, N. S. Pattabiraman, C. J. Lister, T. Grahm *et al.*, *Phys. Rev. C* **75**, 061301(R) (2007).
- [14] C. J. Lister, M. Campbell, A. A. Chishti, W. Gelletly, L. Goettig, R. Moscrop, B. J. Varley, A. N. James, T. Morrison, H. G. Price *et al.*, *Phys. Rev. Lett.* **59**, 1270 (1987).
- [15] T. R. Rodríguez and J. L. Egido, *Phys. Lett. B* **705**, 255 (2011).
- [16] B. Cederwall, F. G. Moradi, T. Bäck, A. Johnson, J. Blomqvist, E. Clément, G. de France, R. Wadsworth, K. Angren, K. Lagergran *et al.*, *Nature (London)* **469** (2011).
- [17] A. M. Romero, J. Dobaczewski, and A. Pastore, *Phys. Lett. B* **795**, 177 (2019).
- [18] W. Satuła and R. Wyss, *Phys. Lett. B* **393**, 1 (1997).
- [19] J. Engel, S. Pittel, M. Stoitsov, P. Vogel, and J. Dukelsky, *Phys. Rev. C* **55**, 1781 (1997).
- [20] G. Martínez-Pinedo, K. Langanke, and P. Vogel, *Nucl. Phys. A* **651**, 379 (1999).
- [21] S. Frauendorf and A. Macchiavelli, *Prog. Part. Nucl. Phys.* **78**, 24 (2014).
- [22] A. L. Goodman, *Phys. Rev. C* **60**, 014311 (1999).
- [23] A. L. Goodman, *Phys. Rev. C* **63**, 044325 (2001).
- [24] K. Kaneko, Y. Sun, and G. de Angelis, *Nucl. Phys. A* **957**, 144 (2017).

- [25] X. Wu, H. Blosser, D. Johnson, F. Marti, and R. C. York, in *Proceedings of the 1999 Particle Accelerator Conference (Cat. No. 99CH36366)* (IEEE, New York, 1999), Vol. 2, pp. 1318–1320, <https://ieeexplore.ieee.org/document/794138>.
- [26] D. J. Morrissey, B. M. Sherrill, M. Steiner, A. Stolz, and I. Wiedenhoever, *Nucl. Instrum. Methods Phys. Res., Sect. B* **204**, 90 (2003).
- [27] D. Bazin, J. Caggiano, B. Sherrill, J. Yurkon, and A. Zeller, *Nucl. Instrum. Methods Phys. Res., Sect. B* **204**, 629 (2003).
- [28] D. Weisshaar, D. Bazin, P. Bender, C. Campbell, F. Recchia, V. Bader, T. Baugher, J. Belarge, M. Carpenter, H. Crawford *et al.*, *Nucl. Instrum. Methods Phys. Res., Sect. A* **847**, 187 (2017).
- [29] J. R. Terry, B. A. Brown, C. M. Campbell, J. M. Cook, A. D. Davies, D.-C. Dinca, A. Gade, T. Glasmacher, P. G. Hansen, B. M. Sherrill *et al.*, *Phys. Rev. C* **77**, 014316 (2008).
- [30] P. Doornenbal, P. Reiter, H. Grawe, T. Saito, A. Al-Khatib, A. Banu, T. Beck, F. Becker, P. Bednarczyk, G. Benzoni *et al.*, *Nucl. Instrum. Methods Phys. Res., Sect. A* **613**, 218 (2010).
- [31] S. A. Milne, M. A. Bentley, E. C. Simpson, P. Dodsworth, T. Baugher, D. Bazin, J. S. Berryman, A. M. Bruce, P. J. Davies, C. A. Diget *et al.*, *Phys. Rev. C* **93**, 024318 (2016).
- [32] P. Adrich, D. Enderich, D. Miller, V. Moeller, R. Norris, K. Starosta, C. Vaman, P. Voss, and A. Dewald, *Nucl. Instrum. Methods Phys. Res., Sect. A* **598**, 454 (2009).
- [33] C. J. Lister, B. J. Varley, H. G. Price, and J. W. Olness, *Phys. Rev. Lett.* **49**, 308 (1982).
- [34] D. Rudolph, C. Baktash, C. J. Gross, W. Satula, R. Wyss, I. Birriel, M. Devlin, H.-Q. Jin, D. R. LaFosse, F. Lerma *et al.*, *Phys. Rev. C* **56**, 98 (1997).
- [35] S. M. Fischer, C. J. Lister, D. P. Balamuth, R. Bauer, J. A. Becker, L. A. Bernstein, M. P. Carpenter, J. Durell, N. Fotiades, S. J. Freeman *et al.*, *Phys. Rev. Lett.* **87**, 132501 (2001).
- [36] A. P. Zuker, A. Poves, F. Nowacki, and S. M. Lenzi, *Phys. Rev. C* **92**, 024320 (2015).
- [37] K. Langanke, D. Dean, and W. Nazarewicz, *Nucl. Phys. A* **728**, 109 (2003).
- [38] M. Hasegawa, K. Kaneko, T. Mizusaki, and Y. Sun, *Phys. Lett. B* **656**, 51 (2007).
- [39] P. Ring and P. Schuck, *The Nuclear Many-Body Problem* (Springer, New York, 2000).
- [40] M. Kortelainen, T. Lesinski, J. Moré, W. Nazarewicz, J. Sarich, N. Schunck, M. V. Stoitsov, and S. Wild, *Phys. Rev. C* **82**, 024313 (2010).
- [41] A. Goodman, *Adv. Nucl. Phys.* **11**, 263 (1979), <https://inis.iaea.org/search/searchsinglerecord.aspx?recordsFor=SingleRecord&RN=11498675>.
- [42] E. Perlińska, S. G. Rohoziński, J. Dobaczewski, and W. Nazarewicz, *Phys. Rev. C* **69**, 014316 (2004).
- [43] K. Sato, J. Dobaczewski, T. Nakatsukasa, and W. Satula, *Phys. Rev. C* **88**, 061301(R) (2013).
- [44] J. A. Sheikh, N. Hinohara, J. Dobaczewski, T. Nakatsukasa, W. Nazarewicz, and K. Sato, *Phys. Rev. C* **89**, 054317 (2014).